Strain field due to point defects in metals

S. K. Rattan, P. Singh, and S. Prakash

Department of Physics, Panjab University, Chandigarh 160 014, India

J. Singh

Department of Physics, Punjab Agricultural University, Ludhiana, Punjab, India

(Received 6 July 1992)

The Kanzaki lattice-statics method is extended to investigate the strain field due to point defects in Al and Cu metals. The dielectric screening method is used to generate host-host and host-impurity interatomic potentials. The Ashcroft-model potential and modified Hartree dielectric function are used for host and impurity atoms. Considering the interactions up to first nearest neighbors (1NN's), the force constants, atomic displacements, and relaxation energy are calculated for substitutional alloys *Al*(Mg,Zn,Sn) and *Cu*(Mg,Zn,Sn). The atomic displacements are calculated up to 20 NN's and these are found to be both positive and negative. The maximum displacement is less than 10% of the interatomic separation. The displacements and relaxation energy in general are smaller in Al alloys than in Cu alloys.

I. INTRODUCTION

The introduction of a point defect in a perfect crystal changes the electrostatic interactions in the vicinity of the point defect. This leads to a change in the atomic force constants. As a result the crystal atoms move to new equilibrium positions and a strain field around the defect is produced.[1-3] Precise knowledge of the strain field is required to study physical properties such as the self-energy of impurity, the electric-field gradient, the residual resistivity, and diffusion, etc.[4-10]

Eshelby[1] has given a complete formulation of the strain field in the continuum model but it overestimates the strain field near the point defect. In this formulation either all the nearest neighbors (NN's) are displaced away from the impurity or towards the impurity causing expansion or contraction around the impurity, which may not be the situation in a metallic crystal due to the presence of conduction electrons.[6-11] In the semidiscrete models,[12-15] the lattice is divided into two regions: In region (a) around the impurity up to a few NN's, the discrete nature of the lattice is accounted for. Region (b) consists of the rest of the crystal which is assumed to be an elastic continuum. The accuracy of these models depends upon the size of region (a).

In the lattice-statics methods, the discrete nature of whole crystal is considered. Both the Kanzaki's method,[6] and the Green's-function method[2-4] are based on the Born–von Kármán model of the crystal. In the Kanzaki method one works with the dynamical equations in the reciprocal space to get the strain field. These are then Fourier inverted to get the strain field in **r** space. The Kanzaki method is extended and used for evaluating the strain field due to vacancy and multiple defects.[16-19] In the Green's-function method one works in **r** space to get the strain field due to point defect. Although both the Kanzaki and Green's-function methods are different in

approach, they are equivalent[3,4] and give elastic continuum results in the asymptotic limit. The computer-simulation calculations[20-22] are performed to estimate the impurity-induced strain field. However, the accuracy depends upon the size of the crystal considered and the choice of the interaction potential.

Most of the calculations, using the methods described above, are done either for a vacancy or an interstitial in simple metals. However, explicit lattice-statics calculations for the substitutional impurity-induced strain field in metals do not exist. This is due to the nonavailability of a reliable host-impurity potential and hence the force constants for the substitutional impurity. In this paper we have generalized Kanzaki's method, which is applicable to different types of point defects in cubic metals. The dielectric screening theory is used to calculate the host-host and host-impurity potentials and hence the strain field.

The plan of this paper is as follows: In Sec. II, the necessary formalism for the impurity-induced strain field is presented. The calculations and results for dilute substitutional alloys of Al and Cu are presented in Sec. III and are discussed in Sec. IV.

II. THEORY

A. General equations of the Kanzaki method

For a perfect crystal with pair potential $\phi(\mathbf{r})$, the total interaction energy Φ_0 is expressed as

$$\Phi_0 = \sum_n \phi(\mathbf{R}_n^0) , \tag{1}$$

where $\mathbf{R}_n^0$ are the equilibrium positions of the host atoms. The introduction of an impurity produces atomic displacements $\mathbf{u}(\mathbf{R}_n^0)$ around itself and thus new equilibrium positions of atoms $\mathbf{R}_n$ are

$$\mathbf{R}_n = \mathbf{R}_n^0 + \mathbf{u}(\mathbf{R}_n^0) \ . \tag{2}$$

Kanzaki assumed that $\mathbf{u}(\mathbf{R}_n^0)$ are produced by an appropriate distribution of external forces (known as Kanzaki forces) in the crystal which depend upon the nature of the impurity. If the impurity is assumed to be at the origin, the total potential energy of the defect lattice in the harmonic approximation is

$$\Phi = \sum_n \phi(\mathbf{R}_n)$$

and

$$\Phi - \Phi_0 = - \sum_{n\alpha} u_\alpha(\mathbf{R}_n^0) F_\alpha(\mathbf{R}_n^0)$$
$$+ \tfrac{1}{2} \sum_{n,n'} \sum_{\alpha,\beta} u_\alpha(\mathbf{R}_n^0) u_\beta(\mathbf{R}_{n'}^0) \phi_{\alpha\beta}(n,n') \ , \tag{3}$$

where

$$F_\alpha(\mathbf{R}_n^0) = - \left[\frac{\partial \phi}{\partial u_{n\alpha}} \right]_{u_{n\alpha}=0} , \tag{4}$$

$$\phi_{\alpha\beta}(n,n') = \left[\frac{\partial^2 \phi}{\partial u_{n\alpha} \partial u_{n'\beta}} \right]_{u_{n\alpha}=0, u_{n'\beta}=0} . \tag{5}$$

α and β ($=1,2,3$) are the Cartesian components. $F_\alpha(\mathbf{R}_n^0)$ is the α component of the external force applied on the atom at $\mathbf{R}_n^0$ and $\phi_{\alpha\beta}(n,n')$ are the force constants which obey the crystal symmetries.[6,23] The equilibrium values of $\mathbf{u}(\mathbf{R}_n^0)$ are obtained by minimizing Φ with respect to $\mathbf{u}(\mathbf{R}_n^0)$, i.e.,

$$\frac{\partial \Phi}{\partial u_\alpha(\mathbf{R}_n^0)} = 0 \ . \tag{6}$$

Substituting Eq. (3) in Eq. (6), one finds

$$F_\alpha(\mathbf{R}_n^0) = \sum_{n',\beta} \phi_{\alpha\beta}(n,n') u_\beta(\mathbf{R}_{n'}^0) \ . \tag{7}$$

Equation (7) shows that the knowledge of $\phi_{\alpha\beta}(n,n')$ and $F_\alpha(\mathbf{R}_n^0)$ is required to evaluate $u_\alpha(\mathbf{R}_n^0)$.

To evaluate $\phi_{\alpha\beta}(n,n')$ in the Fourier space, $\mathbf{u}(\mathbf{R}_n^0)$ is expressed in terms of normal coordinates $\mathbf{Q}(\mathbf{q})$ as

$$\mathbf{u}(\mathbf{R}_n^0) = \sum_{\mathbf{q}} Q(\mathbf{q}) \exp(i\mathbf{q} \cdot \mathbf{R}_n^0) \ , \tag{8}$$

where $\mathbf{q}$ is a wave vector and

$$\mathbf{Q}(-\mathbf{q}) = \mathbf{Q}^*(\mathbf{q}) \ , \tag{9}$$

as $\mathbf{u}(\mathbf{R}_n^0)$ is real. Using Eq. (8) in Eq. (3), one gets

$$\Phi = \Phi_0 - \sum_{\alpha,\mathbf{q}} F_\alpha(\mathbf{q}) Q_\alpha(\mathbf{q})$$
$$+ \frac{N}{2} \sum_{\alpha,\beta} \sum_{\mathbf{q}} \phi_{\alpha\beta}(\mathbf{q}) Q_\alpha(\mathbf{q}) Q_\beta(\mathbf{q}) \ , \tag{10}$$

where

$$F_\alpha(\mathbf{q}) = \sum_n F_\alpha(\mathbf{R}_n^0) \exp(i\mathbf{q} \cdot \mathbf{R}_n^0) \tag{11}$$

and

$$\phi_{\alpha\beta}(\mathbf{q}) = \sum_{n-n'} \phi_{\alpha\beta}(n-n') \exp[-i\mathbf{q} \cdot (\mathbf{R}_{n'}^0 - \mathbf{R}_n^0)] \ . \tag{12}$$

Here N is the number of lattice points. $F_\alpha(\mathbf{q})$ and $\phi_{\alpha\beta}(\mathbf{q})$ are the Fourier transforms of $F_\alpha(\mathbf{R}_n^0)$ and $\phi_{\alpha\beta}(n-n')$, respectively. The equilibrium condition in Fourier space becomes

$$\frac{\partial \Phi}{\partial Q_\alpha(\mathbf{q})} = 0 \ , \tag{13}$$

which in conjunction with Eq. (10) gives

$$\sum_\beta [N\phi_{\alpha\beta}(-\mathbf{q}) Q_\beta(\mathbf{q}) - F_\beta(\mathbf{q}) \delta_{\alpha\beta} \delta_{-\mathbf{q},\mathbf{q}}] = 0 \ . \tag{14}$$

Equation (14) gives three simultaneous equations for three components $Q_\beta(\mathbf{q})$ for each value of $\mathbf{q}$. If $\phi_{\alpha\beta}(\mathbf{q})$ and $F_\beta(\mathbf{q})$ are known, Eq. (14) can be solved for $\mathbf{Q}(\mathbf{q})$ which, in turn, gives $\mathbf{u}(\mathbf{R}_n^0)$ from Eq. (8).

B. Dynamical matrix and Kanzaki forces

The dynamical matrix for a particular structure can be obtained from Eq. (12). If $\phi(\mathbf{r})$ is a central potential, the components $\phi_{\alpha\beta}(n)$ are given as

$$\phi_{\alpha\beta}^{(n)} = \frac{\partial^2 \phi}{\partial r_\alpha \partial r_\beta} \bigg|_{\mathbf{r}=\mathbf{R}_n^0} = \frac{R_{n\alpha}^0 R_{n\beta}^0}{|\mathbf{R}_n^0|^2} (A_n - B_n) + \delta_{\alpha\beta} B_n \ , \tag{15}$$

where

$$A_n = \frac{\partial^2 \phi}{\partial r^2} \bigg|_{\mathbf{r}=\mathbf{R}_n^0}, \quad B_n = \frac{1}{|\mathbf{R}_n^0|} \frac{\partial \phi}{\partial r} \bigg|_{\mathbf{r}=\mathbf{R}_n^0} \ . \tag{16}$$

$R_{n\alpha}^0$ is the α Cartesian component of $\mathbf{R}_n^0$.

In the metallic crystals the ions are screened by the conduction electrons, as a result $\phi(\mathbf{r})$ is long ranged and oscillatory. In d-band metals, the screening is still larger as compared to the simple metals due to partially localized d electrons.[24,25] Therefore, in metallic crystals the major contribution to $\phi_{\alpha\beta}(\mathbf{q})$ and $F_\alpha(\mathbf{q})$ arises from the first NN (1NN) interaction. Retaining only 1NN interactions, $\phi_{\alpha\beta}(\mathbf{q})$ for a fcc crystal is obtained from Eqs. (12) and (15). The explicit expressions are given as

$$\phi_{\alpha\alpha}(\mathbf{q}) = 2(A_1 + B_1) \left\{ 2 - \cos\left[q_\alpha \frac{a}{2}\right] \left[\cos\left[q_\beta \frac{a}{2}\right] + \cos\left[q_\gamma \frac{a}{2}\right] \right] \right\} \tag{17}$$

and

$$\phi_{\alpha\beta}(\mathbf{q})=2(A_1-B_1)\left[\sin\left[q_\alpha\frac{a}{2}\right]\sin\left[q_\beta\frac{a}{2}\right]\right], \tag{18}$$

where $\alpha\neq\beta\neq\gamma$ and a is lattice constant.

For the interactions up to a 1NN shell, $F_\alpha(\mathbf{q})$ for the fcc structure is

$$F_\alpha(\mathbf{q})=i2\sqrt{2}F_I\sin\left[q_\alpha\frac{a}{2}\right]\left[\cos\left[q_\beta\frac{a}{2}\right]+\cos\left[q_\gamma\frac{a}{2}\right]\right], \tag{19}$$

where $\alpha\neq\beta\neq\gamma$ and F_I is the force at the 1NN site defined in Eq. (4). Considering the interaction for the 2NN shell, the components of $\mathbf{F}(\mathbf{q})$ are

$$F_\alpha(\mathbf{q})=i(2F_{II})\sin(q_\alpha a) . \tag{20}$$

Here F_{II} is the force at the 2NN site.

With the knowledge of $F_\alpha(\mathbf{q})$ and $\phi_{\alpha\beta}(\mathbf{q})$, Eq. (14) is solved for $Q_\alpha(\mathbf{q})$ using a simple matrix algebra. For equal radial forces on 12 1NN's of the impurity, $Q_1(\mathbf{q})$ is given as

$$iQ_1=\frac{\sqrt{2}F_I}{A_1N}\begin{vmatrix} \sin x(\cos y+\cos z), & \left[1-\frac{B_1}{A_1}\right]\sin x\sin y, & \left[1-\frac{B_1}{A_1}\right]\sin z\sin x \\ \sin y(\cos z+\cos x), & \left[1+\frac{B_1}{A_1}\right][2-\cos y(\cos z+\cos x)], & \left[1-\frac{B_1}{A_1}\right]\sin y\sin z \\ \sin z(\cos x+\cos y), & \left[1-\frac{B_1}{A_1}\right]\sin y\sin z, & \left[1+\frac{B_1}{A_1}\right][2-\cos z(\cos x+\cos y)] \end{vmatrix}\Bigg/\Delta , \tag{21}$$

where

$$\Delta=\begin{vmatrix} \left[1+\frac{B_1}{A_1}\right][2-\cos x(\cos y+\cos z)], & \left[1-\frac{B_1}{A_1}\right]\sin x\sin y, & \left[1-\frac{B_1}{A_1}\right]\sin z\sin x \\ \left[1-\frac{B_1}{A_1}\right]\sin x\sin y, & \left[1+\frac{B_1}{A_1}\right][2-\cos y(\cos z+\cos x)], & \left[1-\frac{B_1}{A_1}\right]\sin y\sin z \\ \left[1-\frac{B_1}{A_1}\right]\sin z\sin x, & \left[1-\frac{B_1}{A_1}\right]\sin y\sin z, & \left[1+\frac{B_1}{A_1}\right][2-\cos z(\cos x+\cos y)] \end{vmatrix} \tag{22}$$

with $x=aq_1/2$, $y=aq_2/2$, and $z=aq_3/2$.

For equal radial forces on six 2NN's of the impurity, $Q_1(\mathbf{q})$ is

$$iQ_1(\mathbf{q})=\frac{F_{II}}{A_1N}\begin{vmatrix} \sin2x, & \left[1-\frac{B_1}{A_1}\right]\sin x\sin y, & \left[1-\frac{B_1}{A_1}\right]\sin z\sin x \\ \sin2y, & \left[1+\frac{B_1}{A_1}\right][2-\cos y(\cos x+\cos z)], & \left[1-\frac{B_1}{A_1}\right]\sin y\sin z \\ \sin2z, & \left[1-\frac{B_1}{A_1}\right]\sin y\sin z, & \left[1+\frac{B_1}{A_1}\right][2-\cos z(\cos x+\cos y)] \end{vmatrix}\Bigg/\Delta . \tag{23}$$

Q_2 and Q_3 can be obtained from Q_1 using the cubic symmetry.[6] Equations (21) and (23) reduce to those of Kanzaki[6] for $B_1=0$.

C. Model estimation of F_I and F_{II}

For the calculation of the external force $\mathbf{F}(\mathbf{R}_n^0)$ we propose a general model for substitutional and interstitial impurities similar to that for a vacancy.[6] Figure 1 (part A) shows the four configurations for achieving the strain field in the presence of a substitutional impurity. The first three configurations are similar to that of a vacancy[6] except that the strain field produced in configuration (b) is the same as that produced by a substitutional impurity. In configuration (d) the impurity atom is inserted at the vacant lattice site. Figure 1 (part B) shows the configurations for an interstitial impurity.

Let $\phi_{HH}(\mathbf{r})$ and $\phi_{IH}(\mathbf{r})$ be the host-host and impurity-host interaction potentials, respectively. One can write the difference in the potential energies of various consecutive configurations. From Fig. 1 (part A), the energy difference of configurations (d) and (a) is given as

$$\Phi(d)-\Phi(a)=[\Phi(d)-\Phi(c)]+[\Phi(c)-\Phi(b)]+[\Phi(b)-\Phi(a)]$$

$$=\sum_n [\phi_{IH}(|\mathbf{R}_n|)-\phi_{HH}(|\mathbf{R}_n|)]+\tfrac{1}{2}\sum_{n,n'} [\phi_{HH}(|\mathbf{R}_{n'}-\mathbf{R}_n|)-\phi_{HH}(|\mathbf{R}_{n'}^0-\mathbf{R}_n^0|)] . \tag{24}$$

Comparing Eqs. (3) and (24), the second term of both the expressions is the same, therefore the first terms should also be the same. Equating the first terms of Eqs. (3) and (24), the force is given as

$$F_\alpha(\mathbf{R}_n^0)=-\frac{\partial}{\partial u_\alpha(\mathbf{R}_n^0)}\sum_{n'} \Delta\phi(|\mathbf{R}_{n'}|) , \tag{25}$$

where

$$\Delta\phi(\mathbf{r})=\phi_{IH}(\mathbf{r})-\phi_{HH}(\mathbf{r}) . \tag{26}$$

Equation (25) is general and is applicable to various point defects. For an interstitial impurity

(a)

(b)

(c)

(d)

A

(a)

(b)

(c)

B
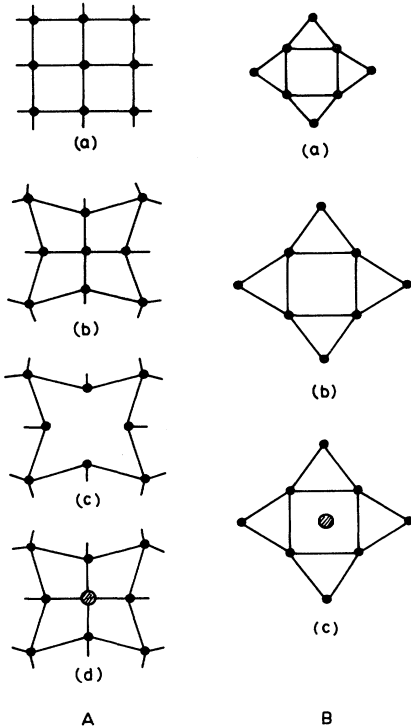
FIG. 1. (Part A) The four configurations of the lattice for substitutional impurity. (a) Perfect host lattice, (b) strained lattice due to external force, (c) strained lattice with one atom removed, and (d) an impurity atom placed at the vacant lattice site. (Part B) The three configurations of the lattice for an interstitial impurity. The description for the (a) and (b) configurations is the same as for part A. In (c), an impurity is inserted at an interstitial site.

$$\Phi(c)-\Phi(a)=\sum_{n_i}' \phi_{IH}(|\mathbf{R}_{n_i}|)$$

$$-\frac{1}{2}\sum_{n,n'} [\phi_{HH}(|\mathbf{R}_{n'}-\mathbf{R}_n|)$$

$$-\phi_{HH}(|\mathbf{R}_{n'}^0-\mathbf{R}_n^0|)] \tag{27}$$

and the equilibrium condition gives

$$F_\alpha(\mathbf{R}_n^0)=-\frac{\partial}{\partial u_\alpha(\mathbf{R}_n^0)}\sum_{n_i}' \phi_{IH}(|\mathbf{R}_{n_i}|) . \tag{28}$$

Here n_i counts the NN's of the interstitial impurity which is assumed at the origin.

To calculate $F_\alpha(\mathbf{R}_n^0)$ for substitutional impurity, $\Delta\phi(\mathbf{r})$ is evaluated in the dielectric screening approach. In a metal the interatomic interaction is written as the sum of direct ion-ion interaction and indirect ion-electron-ion interaction. For the host metal $\phi_{HH}(\mathbf{r})$ is written as[10]

$$\phi_{HH}(\mathbf{r})=\frac{Z_H^2 e^2}{r}+\frac{\Omega_0}{\pi^2}\int F_{HH}(\mathbf{q})\frac{\sin qr}{qr}q^2 dq . \tag{29}$$

Z_H and Ω_0 are the valence and atomic volume of the host metal. $F_{HH}(\mathbf{q})$ is the energy wave-number characteristic function of the host given by[24,25]

$$F_{HH}(\mathbf{q})=\sum_{q'} F_{HH}(\mathbf{q},\mathbf{q}') , \tag{30}$$

where

$$F_{HH}(\mathbf{q},\mathbf{q}')=\frac{\Omega_0 q^2}{8\pi e^2} V_H^b(\mathbf{q})[\bar{\epsilon}_H^1(\mathbf{q},\mathbf{q}')-\delta qq']V_H^b(\mathbf{q}') . \tag{31}$$

Here $V_H^b(\mathbf{q})$ and $\epsilon_H(\mathbf{q},\mathbf{q}')$ are the Fourier transforms of the bare electron-ion potential and dielectric matrix of the host metal, respectively.

In the presence of a substitutional or an interstitial impurity, the overall conduction electron density of the host metal remains practically the same. In other words, it is assumed that the impurity is screened by conduction electrons of the host metal. Therefore, in the presence of the impurity the energy wave-number characteristic function $F_{IH}(\mathbf{q})$ becomes

$$F_{IH}(\mathbf{q})=\sum_{q'} F_{IH}(\mathbf{q},\mathbf{q}') , \tag{32}$$

where

$$F_{IH}(\mathbf{q},\mathbf{q}')=\frac{\Omega_0 q^2}{8\pi e^2} V_I^b(\mathbf{q})[\bar{\epsilon}_H^1(\mathbf{q},\mathbf{q}')-\delta qq']V_H^b(\mathbf{q}') . \tag{33}$$

Here $V_I^b(\mathbf{q})$ is the Fourier transform of bare electron-ion potential for the impurity. The impurity-host interaction potential becomes

$$\phi_{\mathrm{IH}}(\mathbf{r}) = \frac{Z_H Z_I e^2}{|\mathbf{r}|} + \frac{\Omega_0}{\pi^2} \int F_{\mathrm{IH}}(\mathbf{q}) \frac{\sin qr}{qr} q^2 dq \ . \qquad (34)$$

Substituting Eqs. (29) and (34) in Eq. (26), the change in the interatomic potential is given as

$$\Delta\phi(\mathbf{r}) = \frac{\Delta Z Z_H e^2}{|\mathbf{r}|} + \frac{\Omega_0}{\pi^2} \int \Delta F(\mathbf{q}) \frac{\sin qr}{qr} q^2 dq \ , \qquad (35)$$

where $\Delta Z = (Z_I - Z_H)$ is the excess impurity valence. The change in the energy wave-number characteristic function $\Delta F(\mathbf{q})$ is written as

$$\Delta F(\mathbf{q}) = F_{\mathrm{IH}}(\mathbf{q}) - F_{\mathrm{HH}}(\mathbf{q}) \quad \text{for substitutional impurity}$$

$$= -F_{\mathrm{HH}}(\mathbf{q}) \quad \text{for vacancy}$$

$$= F_{\mathrm{IH}}(\mathbf{q}) \quad \text{for interstitial impurity .} \qquad (36)$$

The forces at the 1NN and 2NN sites are calculated with the help of Eqs. (25) and (35). In the central field approximation both the displacements $\mathbf{u}(\mathbf{R}_n^0)$ and forces $\mathbf{F}(\mathbf{R}_n^0)$ are parallel to $\mathbf{R}_n^0$. Therefore, one expands $\Delta\phi(\mathbf{R}_n)$ in Eq. (25) in powers of $u(\mathbf{R}_n^0)$ and gets

$$\mathbf{F}(\mathbf{R}_n^0) = - \frac{\partial}{\partial r} \Delta\phi(\mathbf{r}) \bigg|_{|\mathbf{r}| = |\mathbf{R}_n^0|}$$

$$- u(\mathbf{R}_n^0) \frac{\partial^2}{\partial r^2} \Delta\phi(\mathbf{r}) \bigg|_{|\mathbf{r}| = |\mathbf{R}_n^0|} \ . \qquad (37)$$

If the second term of Eq. (37) is ignored, it is called a first approximation and may be justified only if the displacements are too small as compared to interatomic distances. If both the terms in Eq. (37) are retained, it is called a second approximation. In the first approximation the force constants of the host lattice are unchanged by the presence of the impurity, while the second approximation includes the impurity-induced change in the force constants. The strain field $\mathbf{u}(\mathbf{R}_n)$ in both the first and second approximations can be evaluated using the Kanzaki method.[6]

III. CALCULATIONS AND RESULTS

The formalism developed in Sec. II is used to evaluate the strain field in metallic alloys of Al and Cu. The substitutional impurities Mg, Zn, and Sn are chosen because the electric-field gradient[27] and lattice dilation data in both the Al and Cu matrices are available.[28] In these hosts the dielectric matrix to a fair extent is diagonal, i.e., $\epsilon_{\mathrm{HH}}(\mathbf{q},\mathbf{q}') = \epsilon_H(\mathbf{q})\delta\mathbf{q}\mathbf{q}'$. The effect of the d bands in the Cu host will be discussed later. Thus, $F_{\mathrm{HH}}(\mathbf{q})$ and $F_{\mathrm{IH}}(\mathbf{q})$, in Eqs. (30) and (32) become diagonal. Substituting $F_{\mathrm{HH}}(\mathbf{q})$ and $F_{\mathrm{IH}}(\mathbf{q})$ in Eq. (36), one gets

$$\Delta F(\mathbf{q}) = \frac{\Omega_0 q^2}{8\pi e^2} \Delta V^b(\mathbf{q})[\bar{\epsilon}_H^{-1}(\mathbf{q}) - 1]V_H^b(\mathbf{q}) \ , \qquad (38)$$

where

TABLE I. The physical parameters (in a.u.) of Al, Cu, Mg, Zn, and Sn elements.

Physical parameters	Al	Cu	Mg	Zn	Sn
a	7.637	6.834			
k_f	0.927	0.720			
Ω_0	111.3	79.8			
Z	3	1	2	2	4
r_c	1.12	0.81	1.39	1.27	1.30
A_1	0.0287	0.0038			
B_1	−0.0029	−0.0005			

$$\Delta V^b(\mathbf{q}) = V_I^b(\mathbf{q}) - V_H^b(\mathbf{q}) \ . \qquad (39)$$

$\Delta V^b(\mathbf{q})$ is the excess bare electron-ion potential.

$\Delta F(\mathbf{q})$ can be evaluated if one knows $V_H^b(\mathbf{q})$, $V_I^b(\mathbf{q})$, and $\epsilon_H(\mathbf{q})$. We use the Ashcroft-model potential for both the host and impurity metal ions, its Fourier transform is

$$V^b(q) = -[4\pi Z e^2/q^2]\cos qr_c \ , \qquad (40)$$

where r_c is the potential parameter and Z is the valence. We use a Hartree dielectric function, modified by the Hubbard exchange and correlation correction $f_{\mathrm{xc}}(\mathbf{q})$ given as

$$\epsilon_H(\mathbf{q}) = 1 + \frac{me^2}{\pi\hbar^2 k_f \eta^2}[1 - f_{\mathrm{xc}}(\eta)]$$

$$\times \left[\frac{1}{2} + \left[\frac{1-\eta^2}{4\eta} \right] \ln \left| \frac{1+\eta}{1-\eta} \right| \right] \ , \qquad (41)$$
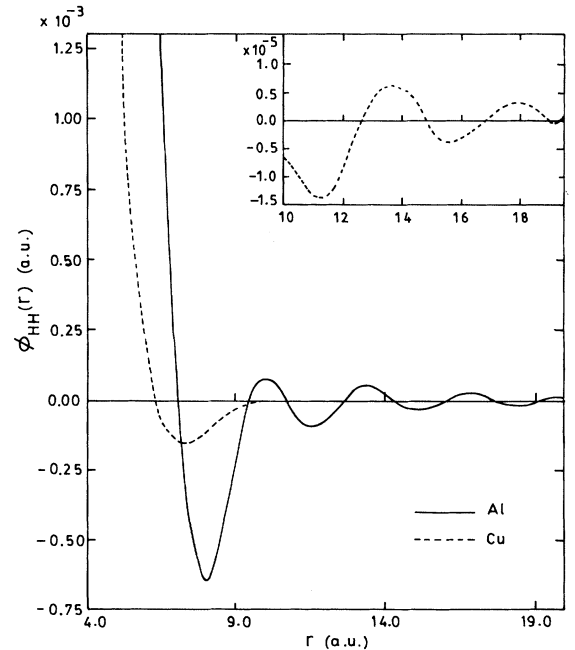
FIG. 2. $\phi_{\mathrm{HH}}(\mathbf{r})$ vs r for Al and Cu metals. The inset is the enlarged view of $\phi_{\mathrm{HH}}(\mathbf{r})$ for Cu at large r.
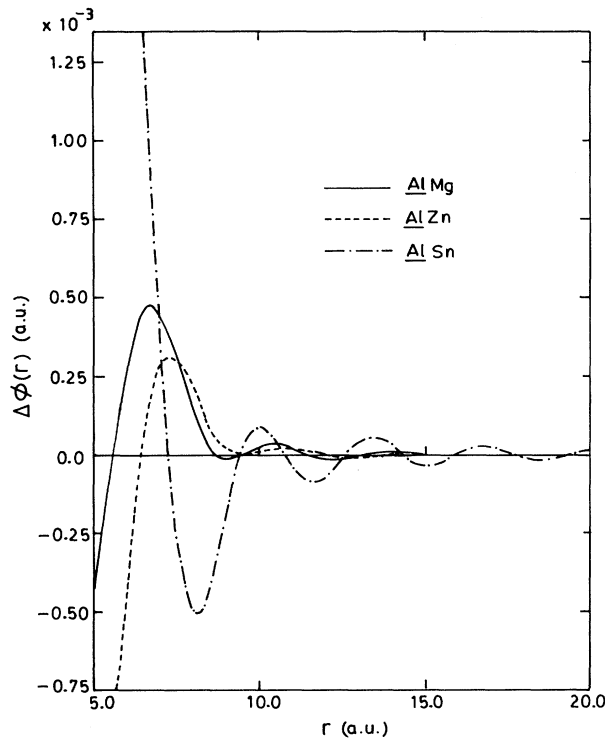
FIG. 3. $\Delta\phi(r)$ vs r for AlMg, AlZn, and AlSn.

FIG. 4. $\Delta\phi(r)$ vs r for CuMg, CuZn, and CuSn. The inset diagram is for $\Delta\phi(r)$ for large r.

where $\eta = q/2k_f$, m is the electronic mass, and k_f is Fermi momentum.

The physical parameters of the host metals and impurities are given in Table I. Figure 2 shows $\phi_{HH}(r)$ versus r for Al and Cu. The magnitude of $\phi_{HH}(r)$ for Al is larger as compared to that for Cu. Further, $\phi_{HH}(r)$ for Al is long ranged as compared to that for Cu due to a larger electron density. At large distances $\phi_{HH}(r)$ exhibits Friedel oscillations for both the metals. The first minimum in $\phi_{HH}(r)$ of the Al metal is at $r = 8.0$ a.u., which is slightly greater than the 2NN distance and is in agreement with Duesbery and Taylor[26] and Singhal.[11] For Cu, $\phi_{HH}(r)$ has the first minimum at $r = 6.85$ a.u., which is again close to the 2NN distance. The calculated parameters A_1 and B_1 are also tabulated in Table I. The magnitude of these parameters for Al is about ten times larger than those for Cu.

The change in potential $\Delta\phi(r)$ as a function of r calculated with the help of Eqs. (35) and (38) for Al and Cu alloys is shown in Figs. 3 and 4, respectively. $\Delta\phi(r)$ exhibits oscillatory behavior at large distances from the impur-

ity. $\Delta\phi(r)$ for AlMg, AlZn, and AlSn are well separated for $r < 10$ a.u. while for large distances $\Delta\phi(r)$ for AlMg and AlZn almost coincide, perhaps due to their same valence. Similar behavior is observed for Cu alloys. $\Delta\phi(r)$ is maximum for AlSn and CuSn alloys. In general, $\Delta\phi(r)$ is proportional to ΔZ. The intercomparison of Figs. 3 and 4 shows that $\Delta\phi(r)$ is larger in magnitude and longer ranged for Al alloys than for Cu alloys for the same impurity.

$\Delta\phi(r)$ is further used to calculate F_I and F_{II} using Eq. (37) for different impurities in Al and Cu. The values of F_I and F_{II} in the second approximation are given in Table II. F_{II} is smaller by an order of magnitude than F_I and it changes sign also for AlZn and AlMg. As expected from Figs. 3 and 4, the Sn impurity produces the maximum force in both hosts.

Using the values of F_I and F_{II}, A_1 and B_1 in Eqs. (21) and (23), the Fourier transforms of the strain fields Q_1, Q_2, and Q_3 are calculated. These values of $Q(\mathbf{q})$ are used in Eq. (8) to obtain $\mathbf{u}(\mathbf{R}_n^0)$ in r space. The numerical calculations are simplified by replacing the summation over

TABLE II. The forces F_I and F_{II} (a.u.) and relaxation energies for Mg, Zn, and Sn impurities in Al and Cu. F_I and F_{II} are in the second approximation.

	Al			Cu		
	Mg	Zn	Sn	Mg	Zn	Sn
$F_I(10^{-3})$	−0.6215	−3.0645	9.4955	5.8739	5.2119	8.2579
$F_{II}(10^{-3})$	0.3456	0.1228	0.8232	0.4791	0.3865	0.8607
$E_r(-eV)$	0.0001	0.0011	0.0093	0.0178	0.0129	0.0339

q by integration over the cube inscribing the first Brillouin zone (BZ) and using the fact that, for any function $F(\mathbf{q})$,

$$\int_{\text{BZ}} F(\mathbf{q})d\mathbf{q} = \frac{1}{4} \int_{\text{cube}} F(\mathbf{q})d\mathbf{q} \qquad (42)$$

for fcc structures. The cube edge is $(4\pi/a)$.[11] The integration is carried out by the Gaussian quadrature method.

The atomic displacements calculated combining the F_I and F_{II} force systems[6] are tabulated in Tables III–V for Mg, Zn, and Sn impurities in Al. We see from Table III–V that all the Mg, Zn, and Sn impurities in Al displace some of the NN's in the outward direction and others in the inward direction, a trend similar to that for a vacancy in Al.[11] If one examines the displacement of the 1NN, one finds that Mg and Zn cause contraction of the Al lattice around the impurity. On the other hand, the Sn impurity causes expansion. Comparison of the atomic displacements caused by a vacancy[11] with those due to a substitutional impurity in Al shows that the strain field produced by a vacancy is much larger than that of a substitutional impurity. Such a behavior is expected as the vacancy produces a larger dilation around itself.

Tables VI–VIII give the atomic displacements due to Mg, Zn, and Sn impurities in the Cu lattice. In the Cu metal these impurities have positive ΔZ. All these impurities produce an expansion of the Cu lattice around themselves. The intercomparison of the atomic displace-

TABLE IV. The displacement components (10^{-2} a.u.) of the NN's of the Zn impurity in Al.

NN's	Displacement components			
(n_1,n_2,n_3)	u_x	u_y	u_z	$\lvert \mathbf{u} \rvert$
110	−1.410	−1.410	0.000	1.994
200	0.276	0.0	0.0	0.276
211	−0.415	−0.339	−0.339	0.634
220	−0.530	−0.530	0.0	0.750
310	0.043	−0.036	0.0	0.056
222	−0.264	−0.264	−0.264	0.458
321	−0.217	−0.201	−0.117	0.318
400	0.052	0.0	0.0	0.052
411	0.015	−0.017	−0.017	0.029
330	−0.242	−0.242	0.0	0.343
420	−0.026	−0.053	0.0	0.059
332	−0.170	−0.170	−0.128	0.272
422	−0.117	−0.091	−0.091	0.173
431	−0.126	−0.123	−0.048	0.183
510	0.025	−0.006	0.0	0.026
521	−0.008	−0.025	−0.012	0.028
440	−0.130	−0.130	0.0	0.184
433	−0.117	−0.101	−0.101	0.185
530	−0.040	−0.050	0.0	0.064
442	−0.109	−0.109	−0.064	0.167
600	0.022	0.0	0.0	0.022
611	0.015	−0.004	−0.004	0.016
532	−0.072	−0.066	−0.046	0.108
620	0.007	−0.010	0.0	0.012
541	−0.081	−0.080	−0.023	0.116

TABLE III. The displacement components (10^{-2} a.u.) of the NN's of the Mg impurity in Al. The coordinates (n_1,n_2,n_3) of NN's are in units of $(a/2)$ here and in the subsequent tables.

NN's	Displacement components			
(n_1,n_2,n_3)	u_x	u_y	u_z	$\lvert \mathbf{u} \rvert$
110	−0.293	−0.293	0.0	0.414
200	0.433	0.0	0.0	0.433
211	−0.069	−0.076	−0.076	0.128
220	−0.107	−0.107	0.0	0.151
310	0.080	0.044	0.0	0.091
222	−0.056	−0.056	−0.056	0.097
321	−0.035	−0.032	−0.016	0.050
400	0.019	0.0	0.0	0.019
411	0.027	0.011	0.011	0.031
330	−0.046	−0.046	0.0	0.065
420	0.019	0.012	0.0	0.022
332	−0.030	−0.030	−0.020	0.047
422	−0.014	−0.010	−0.010	0.020
431	−0.019	−0.017	−0.005	0.026
510	0.009	0.003	0.0	0.010
521	0.010	0.005	0.003	0.011
440	−0.023	−0.023	0.0	0.032
433	−0.018	−0.015	−0.015	0.028
530	0.002	0.001	0.0	0.002
442	−0.017	−0.017	−0.008	0.025
600	0.004	0.0	0.0	0.004
611	0.005	0.001	0.001	0.005
532	−0.008	−0.007	−0.004	0.011
620	0.005	0.002	0.0	0.005
541	−0.011	−0.011	−0.002	0.016

TABLE V. The displacement components (10^{-2} a.u.) of the NN's of the Sn impurity in Al.

NN's	Displacement components			
(n_1,n_2,n_3)	u_x	u_y	u_z	$\lvert \mathbf{u} \rvert$
110	4.344	4.344	0.0	6.143
200	0.563	0.0	0.0	0.563
211	1.342	1.024	1.024	1.974
220	1.645	1.645	0.0	2.327
310	0.134	0.307	0.0	0.335
222	0.809	0.809	0.809	1.401
321	0.704	0.657	0.391	1.039
400	−0.130	0.0	0.0	0.130
411	0.045	0.108	0.108	0.160
330	0.761	0.761	0.0	1.076
420	0.170	0.248	0.0	0.301
332	0.542	0.542	0.421	0.874
422	0.397	0.312	0.312	0.594
431	0.417	0.410	0.167	0.608
510	−0.062	0.035	0.0	0.071
521	0.067	0.113	0.058	0.143
440	0.416	0.416	0.0	0.589
433	0.385	0.334	0.334	0.610
530	0.163	0.195	0.0	0.254
442	0.357	0.357	0.217	0.549
600	−0.070	0.0	0.0	0.070
611	−0.040	0.019	0.019	0.048
532	0.251	0.228	0.161	0.375
620	−0.009	0.047	0.0	0.048
541	0.269	0.269	0.080	0.388

ments caused by the same impurity in Al and Cu shows that the strain field produced in the Cu lattice is much larger than that in the Al lattice. In other words, one can say that the Cu lattice is soft as compared to the Al lattice. This is consistent with the displacements due to vacancy in Al and Cu hosts.[19]

The fractional change in lattice parameters for AlMg, AlZn, and AlSn are 0.099, -0.013, and 0.140, respectively, and for CuMg, CuZn, and CuSn are 0.355, 0.056, and 0.271, respectively.[28] The relative order of magnitude and sign of displacements of 1NN's in Al and Cu alloys shows the same trend as exhibited by the fractional change in the lattice parameter except for AlMg. However, the experimental values of the fractional change in the lattice parameter are estimated from x-ray-diffraction data assuming the lattice as a continuum. Therefore, an exact comparison is not possible. The oscillatory nature of the potential gives the positive and negative displacements of various neighbors. For distant neighbors of the impurity, the magnitude of the displacement goes on decreasing although not in a consistent manner. Suchdev and Tewari[29] obtained the 1NN displacement in the CuFe alloy of the order of -0.006 a.u., which is smaller than the values obtained in our calculations for the Cu alloys. However, it is noted that these displacements are quite sensitive to the choice of interatomic potential.

We have also calculated the relaxation energy E_r defined as

$$E_r = -\frac{1}{2} \sum_{n,\alpha} F_{n\alpha} u_{n\alpha} , \qquad (43)$$

TABLE VII. The displacement components (10^{-2} a.u.) of the NN's of the Zn impurity in Cu.

NN's (n_1, n_2, n_3)	Displacement components			
	u_x	u_y	u_z	$|u|$
110	18.283	18.283	0.0	25.855
200	1.054	0.0	0.0	1.054
211	5.590	4.528	4.528	8.500
220	7.115	7.115	0.0	10.062
310	0.019	1.170	0.0	1.170
222	3.646	3.646	3.646	6.315
321	2.991	2.890	1.737	4.507
400	-0.926	0.0	0.0	0.926
411	-0.142	0.388	0.388	0.566
330	3.362	3.362	0.0	4.755
420	0.475	0.979	0.0	1.088
332	2.448	2.448	1.910	3.954
422	1.670	1.369	1.369	2.557
431	1.796	1.817	0.739	2.659
510	-0.497	0.097	0.0	0.507
521	0.089	0.416	0.206	0.473
440	1.867	1.867	0.0	2.641
433	1.746	1.524	1.524	2.774
530	0.581	0.799	0.0	0.987
442	1.616	1.616	0.981	2.488
600	-0.453	0.0	0.0	0.453
611	-0.332	0.051	0.051	0.340
532	1.049	0.999	0.701	1.609
620	-0.195	0.145	0.0	0.243
541	1.176	1.200	0.350	1.716

TABLE VI. The displacement components (10^{-2} a.u.) of the NN's of the Mg impurity in Cu.

NN's (n_1, n_2, n_3)	Displacement components			
	u_x	u_y	u_z	$|u|$
110	20.594	20.594	0.0	29.125
200	1.586	0.0	0.0	1.586
211	6.315	5.094	5.094	9.580
220	8.017	8.017	0.0	11.338
310	0.097	1.375	0.0	1.379
222	4.105	4.105	4.105	7.110
321	3.379	3.267	1.966	5.095
400	-1.039	0.0	0.0	1.039
411	-0.135	0.453	0.453	0.655
330	3.791	3.791	0.0	5.361
420	0.561	1.129	0.0	1.260
332	2.763	2.763	2.159	4.465
422	1.892	1.553	1.553	2.899
431	2.031	2.055	0.838	3.009
510	-0.558	0.113	0.0	0.569
521	0.113	0.480	0.239	0.548
440	2.107	2.107	0.0	2.980
433	1.973	1.724	1.724	3.137
530	0.666	0.912	0.0	1.129
442	1.827	1.827	1.111	2.813
600	-0.512	0.0	0.0	0.512
611	-0.374	0.059	0.059	0.383
532	1.189	1.133	0.796	1.825
620	-0.217	0.168	0.0	0.274
541	1.330	1.358	0.398	1.942

TABLE VIII. The displacement components (10^{-2} a.u.) of the NN's of the Sn impurity in Cu.

NN's (n_1, n_2, n_3)	Displacement components			
	u_x	u_y	u_z	$|u|$
110	28.908	28.908	0.0	40.882
200	3.942	0.0	0.0	3.942
211	8.941	7.122	7.122	13.468
220	11.264	11.264	0.0	15.930
310	0.463	2.179	0.0	2.228
222	5.753	5.753	5.753	9.965
321	4.788	4.633	2.801	7.227
400	-1.437	0.0	0.0	1.437
411	-0.080	0.709	0.709	1.006
330	5.336	5.336	0.0	7.546
420	0.900	1.696	0.0	1.919
332	3.903	3.903	3.064	6.313
422	2.703	2.223	2.223	4.146
431	2.884	2.923	1.201	4.279
510	-0.775	0.179	0.0	0.795
521	0.211	0.723	0.362	0.835
440	2.975	2.975	0.0	4.208
433	2.800	2.450	2.450	4.455
530	0.983	1.336	0.0	1.659
442	2.591	2.591	1.587	3.993
600	-0.729	0.0	0.0	0.729
611	-0.523	0.090	0.090	0.538
532	1.704	1.624	1.144	2.618
620	-0.294	0.254	0.0	0.389
541	1.891	1.935	0.571	2.765

where $F_{n\alpha}$ are used from Table II and $u_{n\alpha}$ from Tables III–VIII up to 2NN's. In the present model, $\mathbf{F}$ is isotropic. The calculated values are given in Table II. We note that the E_r in the Cu alloys is larger by an order of magnitude than for the Al alloys. The relaxation energy is almost negligible for AlMg.

IV. DISCUSSION

In these calculations the Ashcroft-model potential and modified Hartree dielectric function are used to generate the interatomic potential for the host-host and host-impurity interactions. This description is more justified for Al alloys as the core size of Al is small and the electron density is large. However, in Cu the core size is larger and the d bands of the finite width are near the Fermi energy.[24,25] Therefore, the effect of d electrons would have been considered through $V_H^b(q)$ and $\epsilon_H(\mathbf{q},\mathbf{q}')$. This is an involved calculation and is discussed elsewhere.[30]

The introduction of an impurity changes the charge distribution of the host and hence the dielectric screening function. We have considered this effect only through the bare ion potential and ignored in the dielectric function. It is assumed that it is a higher-order correction and may not affect the results significantly. It was realized that for substitutional impurities the major component of binding energy arises from 1NN's.[27] The interactions therefore are considered only up to 1NN in the evaluation of displacements which is a gross simplification. Singhal[11] has considered interactions up to eight NN's for a vacancy in Al. Our results can be improved by extending these interactions up to higher NN's but this will involve manifold computational efforts. In spite of these simplifications, the present results are useful to estimate other properties of these alloys.

In the elastic continuum model of the lattice the oversized impurity produces expansion of the NN's while the undersized impurity produces the contraction. However, we find from the present calculations that this is not so. The screening field decides the nature of displacements of various NN's. For example, the Zn impurity in Al is an oversized impurity but produces contraction in the lattice. Mg is an undersized impurity in Cu and produces expansion of the Cu lattice. Mg impurity in Al metal causes outward motion for some NN's while inward motion for others. From the above results, we conclude that the nature of the strain field is mainly determined by the electrostatic interactions in the defect lattice.

ACKNOWLEDGMENTS

[1] J. D. Eshelby, in *Solid State Physics,* edited by F. Seitz and D. Turnbull (Acadmic, New York, 1956), Vol. 3, p. 79.

[2] P. A. Flinn and A. A. Maradudin, Ann. Phys. (N.Y.) **18**, 81 (1962).

[3] V. K. Tewary, Adv. Phys. **22**, 757 (1973).

[4] P. T. Heald, in *Vacancies 76,* edited by R. E. Smallman and J. E. Harris (The Metal Society, United Kingdom, 1977), p. 11.

[5] P. H. Dederichs and J. Deutz, *Continuum Models of Discrete Systems* (University of Waterloo Press, Waterloo, 1980), p. 329.

[6] H. Kanzaki, J. Phys. Chem. Solids **2**, 24 (1957).

[7] M. T. Beal-Monod and W. Kohn, J. Phys. Chem. Solids **29**, 1877 (1968).

[8] P. L. Sagalyn and M. N. Alexander, Phys. Rev. B **15**, 5581 (1977).

[9] S. Hafizuddin and N. C. Mohapatra, J. Phys. F **16**, 217 (1986).

[10] W. A. Harrison, *Pseudopotentials in the Theory of Metals* (Benjamin, New York, 1966), p. 23.

[11] S. P. Singhal, Phys. Rev. B **8**, 3641 (1973).

[12] H. B. Huntington, Phys. Rev. **91**, 1092 (1953).

[13] *Calculations of Properties of Vacancies and Interstitial,* Natl. Bur. Std. (U.S.) Misc. Publ. No. 278 (U.S., G.P.O. Washington, D.C., 1966).

[14] M. J. Norgett, J. Phys. C **4**, 1284 (1971).

[15] R. A. Johnson, J. Phys. F **3**, 295 (1973).

[16] J. R. Hardy, J. Phys. Chem. Solids **15**, 39 (1960).

[17] J. R. Hardy and A. B. Lidiard, Philos. Mag. **15**, 825 (1967).

[18] J. R. Hardy and R. Bullough, Philos. Mag. **15**, 237 (1967); **16**, 405 (1967).

[19] R. Bullough and J. R. Hardy, Philos. Mag. **17**, 833 (1968).

[20] I. R. MacGillivray and C. A. Sholl, J. Phys. F **13**, 23 (1983).

[21] L. A. Girifalco and V. G. Weizer, J. Phys. Chem. Solids **12**, 260 (1960).

[22] J. B. Gibson, A. N. Goland, M. Milgram, and G. H. Vineyard, Phys. Rev. **120**, 1229 (1960).

[23] A. A. Maradudin, E. W. Montroll, G . H. Weiss, and I. P. Ipatova, in *Solid State Physics,* edited by H. Ehrenreich, F. Seitz, and D. Turnbull (Academic, New York, 1971), Suppl. 3.

[24] W. Hanke, Phys. Rev. B **8**, 4585 (1973); **8**, 4591 (1973).

[25] J. Singh, N. Singh, and S. Prakash, Phys. Rev. B **12**, 3159 (1975); **12**, 3166 (1975); **18**, 2954 (1978).

[26] M. S. Duesbery and R. Taylor, Phys. Rev. B **7**, 2870 (1973).

[27] B. Pal, S. Mahajan, S. D. Raj, J. Singh, and S. Prakash, Phys. Rev. B **30**, 3191 (1984).

[28] W. B. Pearson, *A Handbook of Lattice Spacings and Structures of Metals and Alloys,* (Pergamon, New York, 1958).

[29] M. Suchdev and V. K. Tewari, J. Phys. F **3**, 1256 (1973).

[30] J. Singh, S. K. Rattan, and S. Prakash, Phys. Rev. B **38**, 10 440 (1988).